

Research Article

Studies of the Influence of Gold Nanoparticles on Characteristics of Mesenchymal Stem Cells

Nataliia Volkova,¹ Olena Pavlovich,² Olena Fesenko,³ Oksana Budnyk,³ Serhii Kovalchuk,³ and Anatoliy Goltsev¹

¹Department of Cryopathophysiology and Immunology, Institute for Problems of Cryobiology and Cryomedicine, The National Academy of Sciences of Ukraine, Pereyaslavskaya Str. 23, Kharkov 61015, Ukraine

²Department of Reproductive Systems, Institute for Problems of Cryobiology and Cryomedicine, The National Academy of Sciences of Ukraine, Pereyaslavskaya Str. 23, Kharkov 61015, Ukraine

³International Surface Enhanced Spectroscopy (SES) Laboratory, Institute of Physics, The National Academy of Sciences of Ukraine, 46 Nauki Ave., Kyiv 03028, Ukraine

Correspondence should be addressed to Nataliia Volkova; volkovannatali2006@yandex.ua

Received 27 July 2017; Accepted 20 September 2017; Published 24 October 2017

Academic Editor: Faheem Ahmed

Copyright © 2017 Nataliia Volkova et al. This is an open access article distributed under the Creative Commons Attribution License, which permits unrestricted use, distribution, and reproduction in any medium, provided the original work is properly cited.

The aim of the present study is to determine what effect the different concentrations of 15 nm gold nanoparticles (AuNPs) will have on the immunophenotype, synthesis collagen type I, ability to direct differentiation and spectroscopic characteristics of bone marrow mesenchymal stem cells (MSCs). The AuNPs in concentrations of 1.5–9 $\mu\text{g/ml}$ did not lead to changes in the level of expression of CD 45, CD 90, and CD 73. It should be noted that AuNPs in concentrations of 6 and 9 $\mu\text{g/ml}$ led to a decrease in CD 44 cells by 6% and 9%, respectively. The content of CD 105 cells was reduced by 5% when AuNPs were applied at a concentration of 9 $\mu\text{g/ml}$. It was found that AuNPs in concentrations of 1.5–6 $\mu\text{g/ml}$ are safe for MSCs, while the increase up to 9 $\mu\text{g/ml}$ has a toxic effect, manifested by the reduction of synthesis collagen type I and ability of adipogenic differentiation. IR spectroscopy data have shown that the AuNPs at concentrations of 9 $\mu\text{g/ml}$ under conditions of adipogenic differentiation to MSCs lead to the destruction processes in the cells. The obtained results are related to the field of applied nanotechnology, which extends to regenerative medicine, especially in development of bioimplantology.

1. Introduction

Nanotechnology involves the design, characterization, and application of structures or systems at the nanometer scale (size range, 1–100 nm) which includes nanofibers, nanotubes, nanogels, and nanoparticles (NPs, e.g., rods, cubes, and spheres) [1–3]. Applications related to engineering, information technology, and diagnostics are examples of consumer applications that directly improve our lives. This technology is intrinsically multidisciplinary and is reliant on techniques and methodologies from many fields such as chemistry, physics, electrical engineering, material science, and molecular biology. Our current knowledge of the health effects of nanomaterials is limited and therefore this aspect deserves

special attention, particularly the potential long-term adverse effects on living organisms [4–6].

The gold nanoparticles (AuNPs) are very attractive for usage in biomedical products due to their unique physical and chemical properties and conventional methods of synthesis [4, 7]. Many approaches to development of medical nanotechnology are based on involvement of metal nanoparticles [8, 9]. These nanoscale metals can have different impact on both physical and chemical properties of cells, depending on their quantity or therapeutic dose [10]. AuNPs are used for cancer targeted therapy and as a contrast agent for biomedical imaging; hence, identification of their possible cytotoxic effects is an important direction of nanobiotechnological research [11, 12].

The impact of metal NPs on stem cells has been scarcely studied so far [3, 13]. Possible interaction could lead to unpredictable consequences in the functioning of organs and tissues as long as all the cells encountered in the primary division of stem cells do not cease to exist. In 2006 the International Society for Cellular Therapy (ISCT) proposed basic criteria for determining MSCs, namely, adhesive fibroblast-like cells that are CD105, CD73, and CD90 positive and CD45, CD34, CD14, or CD11b, CD19, or CD79a and HLA-DR negative, capable of directed differentiation into adipogenic, osteogenic, and chondrogenic lineages. This minimum set of phenotypic criteria for MSCs identification is not associated with their origin [14]. MSCs are normally taken from various tissues, such as bone marrow, fat, and muscles involved in tissue homeostasis and regeneration [15]. We selected bone marrow MSCs of rats as a model object for studying the effect of AuNPs on stem cells. It is likely that mesenchymal stem cells will come into close contact with any AuNPs coated implants. Furthermore, due to their high differentiation capacity, these cells represent an optimal cellular model for analysis of a possible influence of AuNP on cell differentiation. As it has been reported [13] AuNPs have a size-dependent cytotoxicity and NPs less than 15 nm are only considered to be toxic.

Determination of the metal NPs' influence on different types of cultured cells requires evaluation of morphological and functional parameters, namely, viability (membrane integrity) and capacity of adhesion and proliferation [16, 17]. To determine the biosafety and compatibility of metal NPs with cells, most researchers used cytological, biochemical, and biophysical methods. Infrared and Raman spectroscopies are complimentary informative and noninvasive techniques, able to provide the essential information for the diagnosis and evaluation of the cell's functionality without damaging it and use of additional markers [18]. Generic from them is the Single Cell Raman Spectroscopy (SCRS), a label-free method for the analysis of individual parameters of living cells both *in vivo* and *in vitro* [19], because obtained spectrum contains the marker bands (associated with characteristic functional groups) of nucleic acids, proteins, carbohydrates, and lipids, thus reflecting cellular genotypes, phenotypes, and physiological states.

Here we present the study of what effect different concentrations of 15 nm AuNPs will have on the immunophenotype, synthesis collagen type I, ability to direct differentiation and spectroscopic characteristics of bone marrow MSCs.

2. Materials and Methods

2.1. Obtaining and Cultivation of MSCs. MSCs were isolated from resected femur of rats ($n = 7$, weighing 220–225 g) by washing out with Hanks' solution (PAA, Pasching, Austria), followed by flushing through a needle with gradually decreased diameter. The next step was centrifugation at $834 \times g$ for 5 min. The cells were resuspended in culture medium and plated on culture flasks (PAA) with 10^3 cells per cm^2 density. Cultural medium contained: Iscove's Modified Dulbecco's Medium (PAA), 10% fetal bovine serum (FBS)

(HyClone, Logan, UT, USA), gentamicin (150 mg/mL) (Farmak, Kiev, Ukraine), and amphotericin B (10 mg/mL) (PAA). Cultural medium was changed every three days. We used standard culture conditions (37°C , 5% CO_2 , 95% humidity) in a CO_2 incubator (Sanyo, Osaka, Japan). MSCs were detached with 0.25% trypsin-EDTA (Hyclone), which was replanted in other flasks with 1:2 ratios at 80% confluence. Third-passage MSCs were used in all experiments.

2.2. Manipulations with AuNPs. AuNPs were obtained by citrate synthesis [20] with an initial metal concentration of $45 \mu\text{g/mL}$. The average size of AuNPs was 15 nm. The range of investigated concentrations was 1.5, 3, 6, and $9 \mu\text{g/mL}$. AuNPs were introduced in cells by passive diffusion at 37°C . Cells without AuNPs under the same conditions were taken as control ones.

2.3. MSCs Immunophenotyping. For immunophenotypic analysis MSCs after 1 hour incubation with AuNPs were stained with mouse -anti- rat CD45-FITC, CD44-FITC, CD73-FITC, CD90-FITC, and CD105-PE monoclonal antibodies (BD Biosciences, USA) according to the manufacturer's instructions. Measurements were performed on flow cytometer BD FACS Calibur (Becton Dickinson, USA). Data were analyzed using WinMDI v.2.8.

2.4. Immunohistochemical Study of Type I Collagen. Staining for collagen type I was performed using monoclonal antibodies to COL-1 (Sigma-Aldrich, USA) in dilution 1:2000 and CFTM488A (Sigma-Aldrich, USA) according to the manufacturer's instructions. The cells nuclei were additionally stained with DAPI (Sigma-Aldrich, USA) at a concentration of $1 \mu\text{g/mL}$ for 30 min. Fluorescent microscopy of MSCs was performed using confocal scanning microscope LSM 510 Meta (Carl Zeiss, Germany).

2.5. Directed Adipogenic Differentiation. For directed differentiation into adipogenic lineage standard nutrient medium in cultures after reaching confluency was changed for differentiation medium consisting of IMDM, 1% fetal bovine serum, 10^{-7} M dexamethasone, and 10^{-9} M insulin (all from PAA, Austria). Further cultivation was carried out for 3 weeks changing medium twice a week. To confirm the differentiation, the cells were stained with Oil red (Fluka, Germany) and under a light microscope we counted the number of cells with lipid droplets (orange stain), calculating the percentage of the total number of cells. The control ones for spontaneous differentiation were cells cultured without specific inductors.

2.6. Directed Chondrogenic Differentiation. For directed differentiation in chondrogenic lineage, standard nutrient medium in cultures after reaching confluency was changed for differentiation medium consisting of IMDM, 10^{-5} ascorbate-2-phosphate (PAA, Austria), and 10 ng/mL TGF- β (Sigma, USA). Further cultivation was carried out for 3 weeks changing medium twice a week. To confirm the differentiation, the cultures were stained with Toluidine

TABLE 1: Immunophenotype of MSCs after 1 hr incubation with AuNPs.

Sample	Expression level, %				
	CD 44	CD 45	CD 73	CD 90	CD 105
Control	97.7 ± 0.2	1.12 ± 0.11	97.3 ± 0.8	91.5 ± 1.2	95.4 ± 0.4
Au-NPs_1.5 µg/ml	97.2 ± 0.4	0.91 ± 0.12	96.5 ± 0.4	92.1 ± 0.5	93.4 ± 0.3
Au-NPs_3 µg/ml	97.1 ± 0.3	1.07 ± 0.13	96.5 ± 0.3	91.1 ± 0.3	93.1 ± 0.4
Au-NPs_6 µg/ml	92.5 ± 0.4*	1.09 ± 0.08	96.7 ± 0.3	91.3 ± 0.2	93.2 ± 0.5
Au-NPs_9 µg/ml	89.5 ± 0.3*	1.11 ± 0.15	96.5 ± 0.6	91.1 ± 0.1	90.3 ± 0.4*

Note. * $p \leq 0.05$ is significant versus the control.

blue (Fluka, Germany) and we counted the number of cells with proteoglycans in the extracellular matrix (blue stain). Number of differentiated cells was counted under a light microscope and we calculated the percentage of the total number of cells. The control ones for spontaneous differentiation were cells cultured without specific inducers.

2.7. IR Spectroscopy. The spectroscopic characteristics were determined on the 21st day of adipogenic differentiation of MSCs. The IR spectra were acquired in reflection mode on a FTIR Spectrometer VERTEX-70 equipped with Hyperion 1000 Microscope (Bruker). For the data processing the following protocol has been adopted: (1) collecting IR spectrum, (2) baseline correction, (3) spectrum normalization in OH-NH range, (4) spectrum normalization in Amide I range, and (5) spectrum normalization in Amide II region.

2.8. Statistical Analysis. Testing of the normality was carried out using common test for asymmetry and kurtosis. At the normal distribution of variables, reliability of differences between groups was evaluated using Student's *t*-test. Differences are significant at $p \leq 0.05$. Analysis was performed using MS Excel (Microsoft, USA) and Statistica 8 (StatSoft Inc., USA) software.

3. Results and Discussion

3.1. Effect of AuNPs on Immunophenotype of MSCs. MSCs populations derived from bone marrow were characterized by immunophenotype presented in Table 1.

The cells revealed typical mesenchymal phenotype with high expression ($\geq 90\%$) of CD44, CD90, CD105, and CD73 and low expression ($\leq 1\%$) of hematopoietic marker CD45. Addition of the investigated concentrations of AuNPs did not lead to significant changes in the level of expression of CD 45, CD 90, and CD 73.

It should be noted that AuNPs in concentrations of 6 and 9 µg/ml led to a decrease in CD 44 cells by 6% and 9%, respectively. The content of CD 105 cells was reduced by 5% when AuNPs were applied at a concentration of 9 µg/ml. The effect of gold at a concentration of 6 and 9 µg/ml on the decrease in the expression level of the markers CD 44 and CD 105 (9 µg/ml of AuNPs) is probably due to the oppression of the functional state of cells when interacting with nanoparticles. It is known that the CD 44 marker is responsible for the basic functions of the cell, including cell

adhesion, cell homing in peripheral and lymphoid organs and inflammatory foci, cellular activation, and increased production of cytokines and growth factors [21]. When 9 µg/ml of AuNPs was applied, a decrease in the expression of the CD105 (endogen) marker of type I membrane glycoprotein was observed, which functions as an additional receptor for the transforming growth factor beta (TGF- β) superfamily, including TGF- β 1 and TGF- β 3, activin A, and BMP-7. Also, CD 105 is involved in the regulation of migration and the processes of reorganization of the cytoskeleton [14]. These changes in the immunophenotype of the MSC of the bone marrow when interacting with AuNPs give the prerequisites for the detection and prevention of disturbances in the processes of proliferation and differentiation.

3.2. Effect of AuNPs on Synthesis Collagen I Type of MSCs. Morphological characteristics of the studied cells and their ability to produce collagen type I are shown in Figure 1. The control samples of MSCs were characterized by the presence of spindle-shaped and sail-shaped cells, in which $89.6 \pm 2.7\%$ were positively stained for type I collagen. The relative number of cells that synthesized type I collagen, in cultures of MSCs with addition of AuNPs at a concentration of 1.5 and 3 µg/ml, did not differ significantly from the corresponding index in the control and was $87.4 \pm 3.1\%$ and $87.6 \pm 1.9\%$, respectively. The glow in the green region of the spectrum was bright and intense. The use of AuNPs at concentrations of 6 and 9 µg/ml led to a decrease in the relative number of cells positively stained for type I collagen; they were $57.6 \pm 2.1\%$ and $53.4 \pm 2.5\%$, respectively. The luminescence of MSCs cultured with the addition of AuNPs of 9 µg/ml was not intense and covered by small sections of cells (in most cases around the nucleus).

The results of the study of the effect of AuNPs on synthetic processes in MSCs bone marrow showed that the use of concentrations of 6 and 9 µg/ml led to a decrease in the relative number of cells positively stained with collagen type I. As is known, the decrease in the synthetic activity of MSCs of bone marrow is one of the main indicators of attenuation of their functioning [22]. Based on the results of our previous studies, by using confocal laser microscopy of bone marrow MSC culture preparations, it has been shown that low-frequency gold does not remain on the plasma membrane of cells. The localization was partially observed in the cytoplasm and in the cell nucleus [23, 24]. It can be assumed that the AuNPs, by binding to the nucleus cell membrane, have the potential

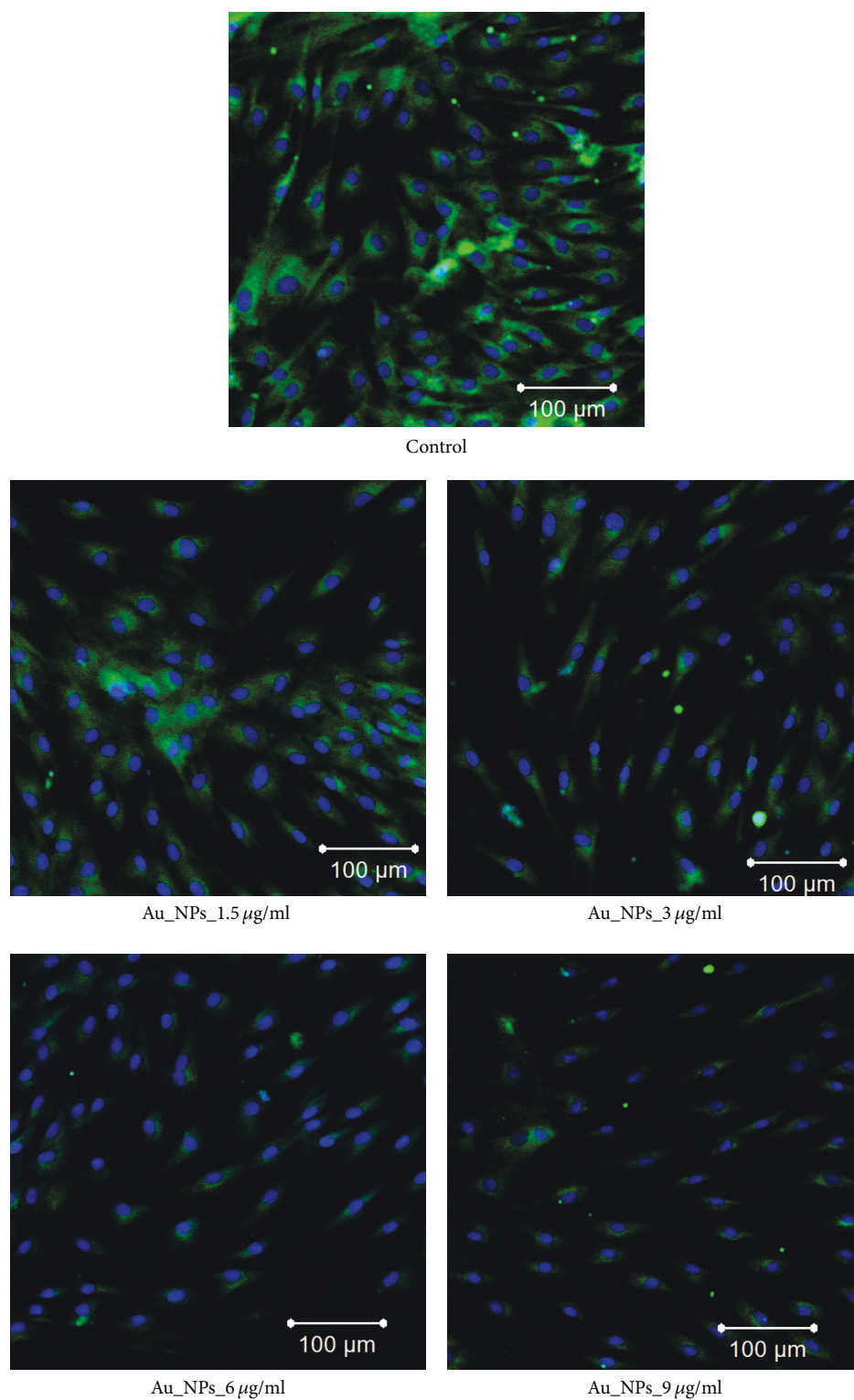


FIGURE 1: The effect of AuNPs on synthesis collagen I type of MSCs, 10th day. Control cells were not incubated with AuNPs. Fluorescent microscopy, immunological staining of MSCs on type I collagen (green light), nucleus stained of DAPI (blue light).

TABLE 2: Ability to direct adipogenic and chondrogenic differentiation of MSCs cultured with addition of AuNPs.

Samples	Adipogenic differentiation, positive staining with Oil red		Chondrogenic differentiation, positive staining with Toluidine blue	
	Spontaneous differentiation	Induced differentiation	Spontaneous differentiation	Induced differentiation
Control	—	+	—	+
Au_NPs_1.5 $\mu\text{g/ml}$	—	+	—	+
Au_NPs_3 $\mu\text{g/ml}$	—	+	—	+
Au_NPs_6 $\mu\text{g/ml}$	—	+	—	+
Au_NPs_9 $\mu\text{g/ml}$	—	±	—	+

Notes. “+”: differentiation of more than 50% cells; “±”: differentiation of less than 50% cells; “—”: no differentiation.

to influence the synthetic processes in the MSCs of the bone marrow at the transcriptional and posttranscriptional levels.

3.3. Effect of AuNPs on Ability to Direct Adipogenic and Chondrogenic Differentiation of MSCs. Ability to direct adipogenic and chondrogenic differentiation of MSCs is presented in Table 2 and Figure 2.

The first signs of adipogenic differentiation, evidenced in changing the morphology of cells (roundness, cytoplasm granularity), were observed on 5–7th day in the case of control samples and at the addition of AuNPs at concentrations of 1.5–6 $\mu\text{g/ml}$.

Application of AuNPs at a concentration of 9 $\mu\text{g/ml}$ inhibited the process of adipogenic differentiation in the cultures studied, which was manifested in the delay in the appearance of the first signs of differentiation, which appeared on 9–10th days. In all investigated concentrations of AuNPs, spontaneous adipogenic differentiation was not observed. Cytochemical staining of MSCs with dye Oil red on 21st day after the initiation of adipocyte differentiation revealed the presence of orange lipid droplets in the cytoplasm of more than $64.7 \pm 6.2\%$ of cells. The use of AuNPs at concentrations of 1.5, 3, and 6 $\mu\text{g/ml}$ did not lead to significant changes in the number of cells with signs of adipogenic differentiation; namely, the index was $64.2 \pm 4.1\%$, $59.7 \pm 5.6\%$, and $61.3 \pm 5.7\%$ of the cells, respectively. In the culture of MSCs with the addition of AuNPs at a concentration of 9 $\mu\text{g/ml}$, the number of cells with signs of adipogenic differentiation was $32.6 \pm 6.5\%$.

In the study of directed chondrogenic differentiation, the first signs of a change in the morphology in the control samples were observed on the 3–4th day of cultivation and on the 5–6th day in the case of using AuNPs in all the concentrations studied. Since the 8th day of chondrogenic differentiation in cultures, we observed areas of high cells concentration. In further observations, cell density increased and on the 21st day there was creation of formed structures with large amount of extracellular matrix, which was confirmed by their staining with Toluidine blue for the proteoglycans. The total percentage of bone marrow cells differentiated in the chondrogenic direction of the control samples was $71.3 \pm 5.2\%$, with the addition of AuNPs of

1.5 $\mu\text{g/ml}$ - $68.7 \pm 7.1\%$, AuNPs of 3 $\mu\text{g/ml}$ - $68.2 \pm 4.8\%$, AuNPs of 6 $\mu\text{g/ml}$ $62.5 \pm 5.3\%$, and AuNPs of 9 $\mu\text{g/ml}$ $62.7 \pm 7.4\%$. In all investigated concentrations of AuNPs, spontaneous chondrogenic differentiation was not observed.

In the studies of authors the effect of AuNPs on direct multilinear differentiation of MSCs was reported [16, 17, 25–28]. Yi et al. reported that uncoated AuNPs decrease the adipogenic differentiation of murine MSCs in a time and dose-dependent manner. The work of Fan et al. showed that although AuNPs had minor cytotoxicity to the cells, they suppressed osteogenic and adipogenic differentiation of hMSCs on days 7 and 14. In our study, we have shown that 15 nm AuNPs led to a decrease in lipid formation in dependency on the applied particle concentration. The MSCs were probably more fragile during adipogenic differentiation; hence, they may constitute a cell system to detect the cytotoxic effects of nanoparticles and other chemical substances [17].

3.4. Spectroscopic Data. With the aim of having more detailed information about how AuNPs influence the cell, the following issues should be addressed: (i) a possible impact of AuNPs on cellular metabolism; (ii) applicability of AuNPs as cellular markers; (iii) an identification of cellular components, which might get affected by AuNPs, for example, lipid membrane or macromolecular nucleic acids (DNA, RNA); and, finally, (iv) which cellular components give maximum contribution to the IR signal from a single cell with AuNPs. Working on solving this puzzle we analyzed the profiles of so-called marker bands of a cell's main components, which are presented in Table 3.

The results of the histochemical study showed no influence of AuNPs on MSCs under chondrogenic differentiation conditions (Table 2). Therefore the next step was to obtain more information about chemical and biochemical changes influenced by AuNPs in MSCs under adipogenic differentiation conditions. We proceeded by performing FTIR spectroscopy of MSCs as such (control set) and those cultivated with AuNPs in concentrations of 1.5, 3, 6, and 9 $\mu\text{g/ml}$ for 21 days of adipogenic differentiations.

The FTIR spectra presented on Figure 3 show a significant increase of the intensity of IR bands from cells with gold concentration of 1.5 $\mu\text{g/ml}$ due to the Surface Enhanced

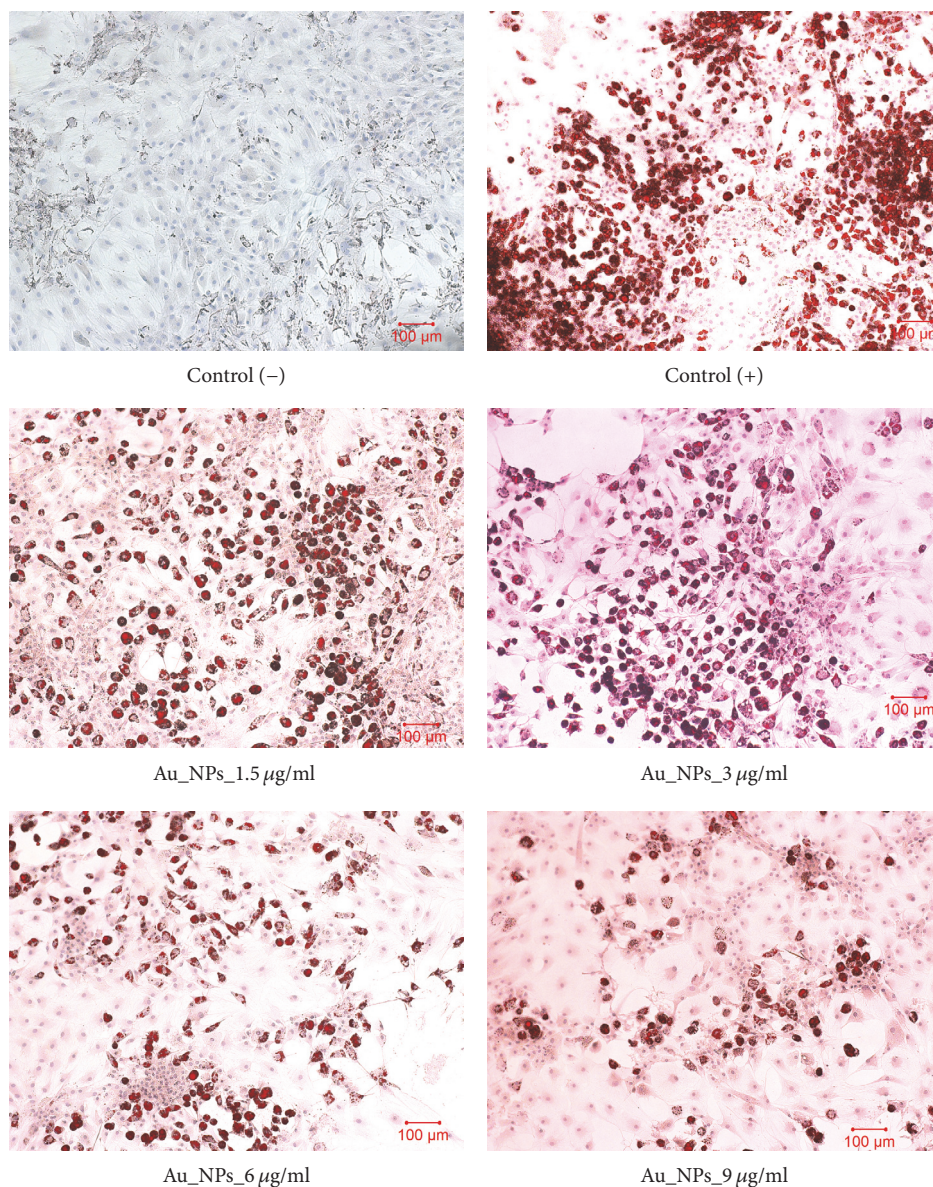


FIGURE 2: The effect of AuNPs on ability of adipogenic differentiation of MSCs, 21st day. Control cells were not incubated with AuNPs. Control (–) cells were not induced to differentiate and control (+) cells were induced to differentiate. Oil red O staining was used to assess adipogenic differentiation by staining for lipid deposits.

TABLE 3: The regions of marker bands for a cell.

Amide I, cm^{-1}	Amide II, cm^{-1}	Nucleic acids, cm^{-1}	νCH_2 , cm^{-1}	νCH_3 , cm^{-1}
1600–1710	1483–1595	1000–1140	2900–2944	2945–2980

Infrared Absorption (SEIRA) effect. In case of SEIRA effect the enhancement of IR absorbance is provided by huge increasing of electromagnetic field in the area around AuNPs. Increase in intensity of IR bands from all cell components, especially enhancement of the signals from the cell nucleus, might indicate that at small concentration of $1.5 \mu\text{g/ml}$ AuNPs mostly pass through the membrane inside the cell. Further increase in gold concentration leads to decrease in IR spectral intensity, which is probably caused by excessive deposition of

AuNPs and cluster's formation of that on a cell membranes. In this case AuNPs still remain a good enhancement factor for cell membrane, which is revealed in strong lipid peaks, but prevent obtaining a good signal from the cell as a whole.

The results of analysis of the intensities of absorption bands of Amide I and Amide II in the IR spectra, which have been measured on the samples of cell cultures with directed adipogenic differentiation and different concentrations of AuNPs are given in Table 4. In the studied samples, the

TABLE 4: Calculated value of Amide I/Amide II ratio in MSC of bone marrow under adipogenic differentiation conditions.

Sample	IR band for Amide I		IR band for Amide II		Amide I/Amide II	Standard deviation
	Position, cm^{-1}	Intensity, a.u.	Position, cm^{-1}	Intensity, a.u.		
Control (no AuNPs)	1645	0.126	1541	0.095	1.309	± 0.0007
Au_NPs_1.5 $\mu\text{g/ml}$	1646	0.46	1545	0.38	1.269	± 0.0007
Au_NPs_3 $\mu\text{g/ml}$	1645	0.196	1541	0.14	1.255	± 0.0007
Au_NPs_6 $\mu\text{g/ml}$	1645	0.11	1536	0.095	1.408	± 0.0007
Au_NPs_9 $\mu\text{g/ml}$	1642	0.14	1536	0.11	1.422	± 0.0007

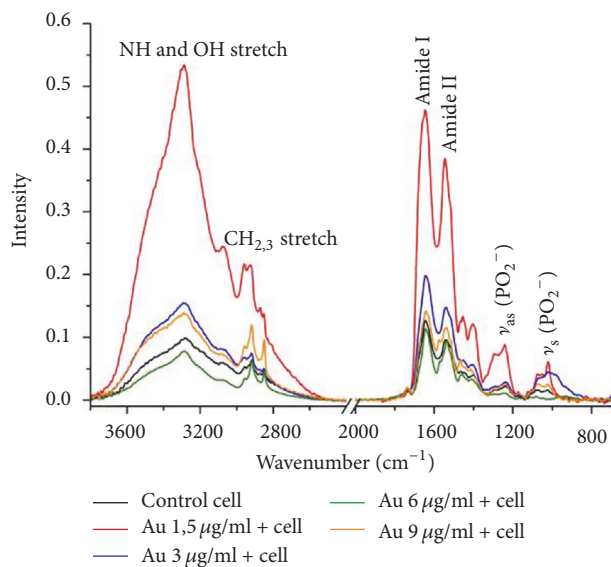


FIGURE 3: FTIR spectra of pristine MSCs (labeled as control cell, black) and of MSCs incubated with AuNPs in concentrations of 1.5 (red), 3 (blue), 6 (green), and 9 (magenta) $\mu\text{g/ml}$ for 21 days of adipogenic differentiations. Resolution 2 cm^{-1} ; 234 scans are collected. The spectra background are subtracted.

Amide I/Amide II ratio was higher by 7% and 8% for samples of AuNPs with concentrations of 6 and 9 $\mu\text{g/ml}$, respectively, as compared to the corresponding reference indicator. This points to the necessity of taking into account the specific biochemical changes inherent to each process of differentiation when assessing the nature of the change in Amide vibrations as an apoptotic marker [25].

The ratios between the signals in the $2853\text{--}2291\text{ cm}^{-1}$ region (absorption of CH_2 groups) and in the $2945\text{--}2980\text{ cm}^{-1}$ region (absorption of CH_3 groups) were analyzed. An increase of the CH_2/CH_3 ratio is observed during the cells growth in one type of cell culture. The results presented in [29] showed that changes were observed in the ratio of CH_2/CH_3 in the process of cell growth and are not the only characteristic of apoptosis.

The IR spectrum presented on Figure 4 and in Table 5 shows the ratio of asymmetric stretching modes of CH_2/CH_3 hydrocarbon functional groups as markers of apoptosis in cells with directed adipogenic differentiation. In this case, the ratio of CH_2/CH_3 asymmetric modes increases with the rise

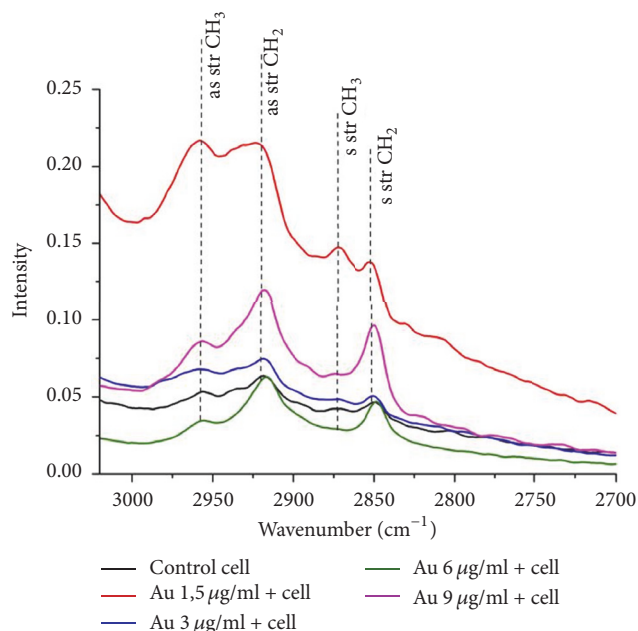


FIGURE 4: FTIR spectra of pristine MSCs (labeled as control cell, black) and of MSCs incubated with AuNPs in concentrations of 1.5 (red), 3 (blue), 6 (green), and 9 (magenta) $\mu\text{g/ml}$ for 21 days of adipogenic differentiations enlarged in the region of CH vibrations. Resolution 2 cm^{-1} ; 232 scans are collected. The spectra background are subtracted.

of the AuNPs concentration and most sufficient growth is observed at concentration of 9 $\mu\text{g/ml}$.

The experimental data obtained regarding the change in the CH_2/CH_3 ratio are not fully understood and, therefore, cannot be considered as characteristic of apoptosis. On the contrary, they may be associated with an increase in the number of lipids in the secondary messenger that regulates cell growth. Another explanation is the possible reduction of the cell volume and, hence, of the actual number of molecules with CH_2/CH_3 during the cell growth and are not the only characteristic features of apoptosis [30].

It is important to note that IR spectroscopy does not damage the cells and provides both qualitative and quantitative information related to proteins, lipids, and nucleic acids of living, necrotic, or apoptotic cells within one experimental point without manipulation or staining of the sample.

The molecular mechanism behind the increase in the CH_2/CH_3 ratio is still unclear, but this may be due to an

TABLE 5: Ratio of intensities of asymmetric bands CH_2/CH_3 in MSCs under conditions of adipogenic differentiation.

Sample	IR band for CH_2 (as)		IR band for CH_3 (as)		Ratio of CH_2/CH_3	Standard deviation
	Position, cm^{-1}	Intensity, a.u.	Position, cm^{-1}	Intensity, a.u.		
Control (no AuNPs)	2921	0.123	2956	0.082	1.502	± 0.0006
Au_NPs_1.5 $\mu\text{g}/\text{ml}$	2921	0.087	2960	0.076	1.513	± 0.0006
Au_NPs_3 $\mu\text{g}/\text{ml}$	2917	0.058	2956	0.043	1.531	± 0.0006
Au_NPs_6 $\mu\text{g}/\text{ml}$	2921	0.044	2956	0.040	1.547	± 0.0006
Au_NPs_9 $\mu\text{g}/\text{ml}$	2921	0.037	2957	0.032	1.762	± 0.0006

increase in the number of lipids in the secondary messenger that regulates cell growth or a slight decrease in cell volume after the cells have grown. Indeed, the decrease in the volume of cells corresponds to a relative increase in surface area. This can lead to an increase in the proportion of phospholipids in biomass and, respectively, a major increase in CH_2 in relation to CH_3 groups.

Thus, based on the IR spectroscopy data, it has been established that the AuNPs at concentrations of 1.5–6 $\mu\text{g}/\text{ml}$ do not affect the structure of the MSC of the bone marrow. It is shown that the addition of the AuNPs at concentrations of 9 $\mu\text{g}/\text{ml}$ under conditions of adipogenic differentiation to MSCs of the bone marrow leads to the formation of the Amide I shoulder in the region of 1617–1630 cm^{-1} [31, 32], increasing lipid content; appearance of intensive peak at 1740 cm^{-1} , which is usually associated with the non-hydrogen-bonded ester carbonyl $\text{C}=\text{O}$ stretching mode within phospholipids; and increasing the shoulder at $\sim 1725 \text{ cm}^{-1}$ which is associated with hydrogen-bonded $\text{C}=\text{O}$ groups. An increase in a peak at $\sim 1725 \text{ cm}^{-1}$ was seen by [33] for investigated cells that had experienced necrosis and was visually changed morphologically because of a loss of cell membrane integrity. The results are likely to indicate the destruction processes in the studied cells. The fact that the $\sim 1740 \text{ cm}^{-1}$ peak in Figure 3 is significantly more intense than the $\sim 1725 \text{ cm}^{-1}$ peak implies that the $\text{C}=\text{O}$ ester carbonyl groups of lipids in the cell are becoming predominantly non-hydrogen-bonded, which would be in agreement with oxidative damage having occurred. Apoptosis is associated with, among other factors, increased oxidative damage [34, 35]. Therefore, the cells with the AuNPs at concentrations of 9 $\mu\text{g}/\text{ml}$ that we measured may have been in the early stages of apoptosis and not a lysosomal type of death whereas cells visually observed to have lost membrane integrity were most likely lysosomal and had different IR spectral characteristics.

4. Conclusions

It was shown that the use of AuNPs in concentration of 1.5–9 $\mu\text{g}/\text{ml}$ did not lead to significant changes in the level of expression of CD 45, CD 90, and CD 73. It should be noted that AuNPs in concentrations of 6 and 9 $\mu\text{g}/\text{ml}$ led to a decrease in CD 44 cells by 6% and 9%, respectively. The content of CD 105 cells was reduced by 5% when AuNPs were applied at a concentration of 9 $\mu\text{g}/\text{ml}$. It was found that AuNPs in concentration of 1.5–6 $\mu\text{g}/\text{ml}$ are safe for MSCs, while increase up to 9 $\mu\text{g}/\text{ml}$ has a toxic effect,

manifested by the reduction of synthesis collagen type I, adipogenic differentiation ability, and apparent apoptosis. IR spectroscopy data have shown that the AuNPs at concentrations of 1.5–6 $\mu\text{g}/\text{ml}$ do not affect the structure of proteins, lipids, and nucleic acids of the MSC of the bone marrow. The addition of the AuNPs at concentrations of 9 $\mu\text{g}/\text{ml}$ under conditions of adipogenic differentiation to MSCs leads to the destruction processes in the cells. The obtained results are related to the field of applied nanotechnology, which extends to regenerative medicine, especially in development of bioimplantology.

Conflicts of Interest

The authors declare that they have no conflicts of interest.

Authors' Contributions

Anatoliy Goltsev and Nataliia Volkova contributed to study design; Nataliia Volkova and Olena Pavlovich performed the experiments of cultivation and differentiation of MSCs, analyzed the data, and wrote the manuscript; Olena Fesenko performed analysis of results of IR study of MSCs and participated in writing the manuscript; Oksana Budnyk and Serhii Kovalchuk measured IR spectra of MSCs and analysis of resulting IR spectra.

Acknowledgments

The work was carried out within the research project of Marie Curie ILSES FP7, Projects 612620 and N70/17-H National Academy of Sciences of Ukraine.

References

- [1] Y. Teow, P. V. Asharani, M. P. Hande, and S. Valiyaveetil, "Health impact and safety of engineered nanomaterials," *Chemical Communications*, vol. 47, no. 25, pp. 7025–7038, 2011.
- [2] A. M. Alkilany and C. J. Murphy, "Toxicity and cellular uptake of gold nanoparticles: what we have learned so far?" *Journal of Nanoparticle Research*, vol. 12, no. 7, pp. 2313–2333, 2010.
- [3] E. Söderstjerna, F. Johansson, B. Klefbohm, and U. Englund Johansson, "Gold- and silver nanoparticles affect the growth characteristics of human embryonic neural precursor cells," *PLoS ONE*, vol. 8, no. 3, Article ID e58211, 2013.
- [4] N. Khlebtsov and L. Dykman, "Biodistribution and toxicity of engineered gold nanoparticles: a review of in vitro and in vivo

- studies," *Chemical Society Reviews*, vol. 40, no. 3, pp. 1647–1671, 2011.
- [5] G. V. Lowry, K. B. Gregory, S. C. Apte, and J. R. Lead, "Transformations of nanomaterials in the environment," *Environmental Science & Technology*, vol. 46, no. 13, pp. 6893–6899, 2012.
 - [6] A. Bour, F. Mouchet, J. Silvestre, L. Gauthier, and E. Pinelli, "Environmentally relevant approaches to assess nanoparticles ecotoxicity: A review," *Journal of Hazardous Materials*, vol. 283, pp. 764–777, 2015.
 - [7] N. G. Khlebtsov, A. G. Melnikov, L. A. Dykman, and V. A. Bogatyrev, "Optical properties and biomedical applications of nanostructures based on gold and silver bioconjugates, photopolarimetry in remote sensing," *Photopolarimetry in Remote Sensing*, pp. 265–308, 2004.
 - [8] J. G. Leu, S. A. Chen, H. M. Chen et al., "The effects of gold nanoparticles in wound healing with antioxidant epigallocatechin gallate and alpha-lipoic acid," *Nanomedicine: Nanotechnology, Biology and Medicine*, vol. 8, no. 5, pp. 767–775, 2012.
 - [9] N. Volkova, M. Yukhta, O. Pavlovich, and A. Goltsev, "Application of cryopreserved fibroblast culture with au nanoparticles to treat burns," *Nanoscale Research Letters*, vol. 11, no. 1, article no. 22, pp. 1–6, 2016.
 - [10] R. Cao-Milán and L. M. Liz-Marzán, "Gold nanoparticle conjugates: recent advances toward clinical applications," *Expert Opinion on Drug Delivery*, vol. 11, no. 5, pp. 741–752, 2014.
 - [11] R. Arvizo, R. Bhattacharya, and P. Mukherjee, "Gold nanoparticles: opportunities and challenges in nanomedicine," *Expert Opinion on Drug Delivery*, vol. 7, no. 6, pp. 753–763, 2010.
 - [12] J. P. M. Almeida, A. L. Chen, A. Foster, and R. Drezek, "In vivo biodistribution of nanoparticles," *Nanomedicine*, vol. 6, no. 5, pp. 815–835, 2011.
 - [13] Y. Pan, S. Neuss, A. Leifert et al., "Size-dependent cytotoxicity of gold nanoparticles," *Small*, vol. 3, no. 11, pp. 1941–1949, 2007.
 - [14] M. Dominici, K. Le Blanc, I. Mueller et al., "Minimal criteria for defining multipotent mesenchymal stromal cells. the international society for cellular therapy position statement," *Cytotherapy*, vol. 8, no. 4, pp. 315–317, 2006.
 - [15] H. Busser, M. Najar, G. Raicevic et al., "Isolation and characterization of human mesenchymal stromal cell subpopulations: comparison of bone marrow and adipose tissue," *Stem Cells and Development*, vol. 24, no. 18, pp. 2142–2157, 2015.
 - [16] S. J. Soenen, B. Manshian, J. M. Montenegro et al., "Cytotoxic effects of gold nanoparticles: A multiparametric study," *ACS Nano*, vol. 6, no. 7, pp. 5767–5783, 2012.
 - [17] Y. Kohl, E. Gorjup, A. Katsen-Globa, C. Büchel, H. Von Briesen, and H. Thielecke, "Effect of gold nanoparticles on adipogenic differentiation of human mesenchymal stem cells," *Journal of Nanoparticle Research*, vol. 13, no. 12, pp. 6789–6803, 2011.
 - [18] K. Ataka and J. Heberle, "Functional vibrational spectroscopy of a cytochrome c monolayer: SEIDAS probes the interaction with different surface-modified electrodes," *Journal of the American Chemical Society*, vol. 126, no. 30, pp. 9445–9457, 2004.
 - [19] M. Li, J. Xu, M. Romero-Gonzalez, S. A. Banwart, and W. E. Huang, "Single cell Raman spectroscopy for cell sorting and imaging," *Current Opinion in Biotechnology*, vol. 23, no. 1, pp. 56–63, 2012.
 - [20] A. D. McFarland, C. L. Haynes, C. A. Mirkin, R. P. Van Duyne, and H. A. Godwin, "Color my nanoworld," *Journal of Chemical Education*, vol. 81, no. 4, p. 544A, 2004.
 - [21] D. Baksh, R. Yao, and R. S. Tuan, "Comparison of proliferative and multilineage differentiation potential of human mesenchymal stem cells derived from umbilical cord and bone marrow," *Stem Cells*, vol. 25, no. 6, pp. 1384–1392, 2007.
 - [22] J. P. Rodríguez, L. Montecinos, S. Ríos, P. Reyes, and J. Martínez, "Mesenchymal stem cells from osteoporotic patients produce a type I collagen-deficient extracellular matrix favoring adipogenic differentiation," *Journal of cellular biochemistry*, vol. 79, no. 4, pp. 557–565.
 - [23] N. Volkova, O. Pavlovich, O. Fesenko, O. Budnyk, and A. Goltsev, "Influence of gold nanoparticles on morphological and functional characteristics of bone marrow mesenchymal stem cells: MTT assays and spectroscopic data," *Nano Studies*, vol. 14, pp. 151–160, 2016.
 - [24] E. V. Pavlovich and N. A. Volkova, "Influence of gold nanoparticles on human fibroblast before and after cryopreservation," in *Nanoplasmonics, Nano-Optics, Nanocomposites, and Surface Studies*, vol. 167 of *Springer Proceedings in Physics*, pp. 413–420, Springer International Publishing, Basel, Switzerland, 2015.
 - [25] C. Yi, D. Liu, C.-C. Fong, J. Zhang, and M. Yang, "Gold nanoparticles promote osteogenic differentiation of mesenchymal stem cells through p38 MAPK pathway," *ACS Nano*, vol. 4, no. 11, pp. 6439–6448, 2010.
 - [26] J. H. Fan, W. I. Hung, and J. M. Yeh, "Biocompatibility study of gold nanoparticles to human cells," *ICBME Proceedings*, 2009.
 - [27] J. Fan, W. Li, W. Hung, C. Chen, and J. Yeh, "Cytotoxicity and differentiation effects of gold nanoparticles to human bone marrow mesenchymal stem cells," *Biomedical Engineering : Applications, Basis, and Communications*, vol. 23, no. 02, pp. 141–152, 2011.
 - [28] L. M. Ricles, S. Y. Nam, K. Sokolov, S. Y. Emelianov, and L. J. Suggs, "Function of mesenchymal stem cells following loading of gold nanotracers," *International Journal of Nanomedicine*, vol. 6, pp. 407–416, 2011.
 - [29] X. Zhang, "Gold nanoparticles: recent advances in the biomedical applications," *Cell Biochemistry and Biophysics*, vol. 72, no. 3, pp. 771–775, 2015.
 - [30] W. Zhou, X. Gao, D. Liu, and X. Chen, "Gold Nanoparticles for in vitro diagnostics," *Chemical Reviews*, vol. 115, no. 19, pp. 10575–10636, 2015.
 - [31] Y. Gao, X. Huo, L. Dong et al., "Fourier transform infrared microspectroscopy monitoring of 5-fluorouracil-induced apoptosis in SW620 colon cancer cells," *Molecular Medicine Reports*, vol. 11, no. 4, pp. 2585–2591, 2015.
 - [32] H. Y. Holman, M. C. Martin, E. A. Blakely, K. Bjornstad, and W. R. McKinney, "IR spectroscopic characteristics of cell cycle and cell death probed by synchrotron radiation based Fourier transform IR spectromicroscopy," *Biopolymers*, vol. 57, no. 6, pp. 329–335.
 - [33] N. Jamin, P. Dumas, J. Moncuit et al., "Highly resolved chemical imaging of living cells by using synchrotron infrared microspectrometry," *Proceedings of the National Academy of Sciences of the United States of America*, vol. 95, no. 9, pp. 4837–4840, 1998.
 - [34] R. Mittler and A. Y. Cheung, *When Cells Die II: A Comprehensive Evaluation of Apoptosis and Programmed Cell Death*, Wiley, New York, NY, USA, 2004.
 - [35] R. Birge, *When Cells Die II: A Comprehensive Evaluation of Apoptosis and Programmed Cell Death*, John Wiley and Sons, Inc., New York, NY, USA, 2003.

